

The structure of surfaces: what do we know and what would we like to know?

This article has been downloaded from IOPscience. Please scroll down to see the full text article.

2010 J. Phys.: Condens. Matter 22 084016

(<http://iopscience.iop.org/0953-8984/22/8/084016>)

View [the table of contents for this issue](#), or go to the [journal homepage](#) for more

Download details:

IP Address: 129.252.86.83

The article was downloaded on 30/05/2010 at 07:15

Please note that [terms and conditions apply](#).

The structure of surfaces: what do we know and what would we like to know?

D P Woodruff

Physics Department, University of Warwick, Coventry CV4 7AL, UK

Received 11 March 2009, in final form 19 March 2009

Published 5 February 2010

Online at stacks.iop.org/JPhysCM/22/084016

Abstract

A brief survey is presented of the methods of quantitative surface structure determination and some of the main phenomena that have been established, and their associated trends. These include surface relaxation and reconstruction of clean surfaces and the structures formed by atomic and molecular adsorbates. Examples include the surfaces of semiconductors, oxides and metals. Future challenges, concerned with complexity and precision, are discussed.

(Some figures in this article are in colour only in the electronic version)

1. Introduction

Understanding the structure of surfaces, i.e. the exact location of atoms in the near-surface region, is a key starting point to understanding many of the electronic and chemical properties of surfaces. It is now approaching 40 years since the first quantitative experimental surface structure determinations were performed using low energy electron diffraction (LEED) (e.g. [1, 2]), and in that time our knowledge of surface structure has increased enormously. The systematics of the way in which the structure of clean surfaces differs from that of the underlying bulk are well understood, in most cases at a good quantitative level, and clear patterns have emerged in the local adsorption site and chemisorption bondlengths for most atomic, and many molecular, adsorbates on surfaces that are also, in large part, understood in considerable detail. Advances in the effectiveness of modern computer programs based on density functional theory (DFT), and in the amount of readily available computing power, also means that some quite subtle effects in surface structural modifications can be reproduced by these total energy calculations to determine the minimum energy structure. Indeed, the success of this approach is such that an emerging trend in surface structural research is to replace quantitative experiments by these purely theoretical simulations; historically, the starting point for electronic structure calculations was a knowledge of the structure, but now the computational methods allow one to optimize the structure first. Why then, some argue, bother with the experiments at all? The clear answer is that there are enough examples of failures in the application of DFT to obtain the correct surface structure (sometimes only in subtle differences in bondlengths, sometimes in the basic structural model) to highlight the continuing need for proper experimental

determinations. Such failures may not be common, but with no generally-accepted way of predicting when they will occur, they present an important problem. Nevertheless, there is an important role for both experiment and theory, not least because while experiment may provide correct and precise structural information, if theoretical calculations lead to the same energetically-favoured structure, one then has the possibility to ‘unpick’ the details of theoretical calculations in order to understand why this is the favoured structure.

In this short review my objective is to give an overview of the present state of knowledge of surface structure phenomenology and to put the past achievements and future challenges in the context of the limitations imposed by the available experimental and theoretical methods.

2. Experimental and theoretical methods

While a detailed account of the many methods used in surface structure determination is clearly beyond the scope of this paper, an appreciation of a few key aspects of the methods is important to put the results of their application in perspective. The main experimental methods yielding quantitative structural information fall into one of two groups, those that rely on wave-interference in elastic scattering of electrons and photons, and methods based on ion scattering. In the first category is a subdivision into conventional diffraction, that relies on long-range order, and local scattering methods that rely only on local order. In addition some comments on atomic-scale imaging, and on the use of theoretical (mainly DFT) total energy calculations, are included.

The first quantitative surface structure determinations were obtained by low energy electron diffraction (LEED) [3, 4], and this method has still yielded the largest number of such

structural solutions [5]. This is a conventional crystallographic diffraction method, much like x-ray diffraction, but the strong elastic and inelastic scattering experienced by electrons in the energy range of $\sim 30\text{--}300$ eV ensures that the detected diffracted beam intensities derive entirely from the outermost few atomic layers, with a typical attenuation length of the order of two atomic layers. This intrinsic surface specificity makes LEED a natural choice for studying surfaces, but also leads to a complication in interpretation, because the strong elastic scattering means that multiple scattering of the electrons by different atoms in the surface (so-called dynamical effects) is very important and must be included in theoretical simulations of the diffracted beam intensities. Structure determination is therefore achieved by comparing the measured intensities with those simulated for a sequence of trial model structures, the best-fit structure (as judged by an objective reliability- or R -factor) being deemed to be the correct structure. Clearly this ‘trial-and-error’ approach to obtaining the structural solution is a potential limitation, both because of the time it may take to optimize the structural parameter values for a correct structural model, but also because the correct structure can be found only if the correct basic model is tested. This limitation, however, is not unique to LEED—it is a feature of almost all methods of surface structure determination, including those based on DFT total energy calculations. Historically, the computational demands of the multiple scattering simulations required for a LEED structure analysis presented a significant limitation to the method, but the current availability of relatively low cost, high speed, computing has greatly reduced this problem, although structures with a large surface periodicity remain challenging.

The alternative diffraction method is to use x-rays [6, 7]. In this case, the atomic scattering cross-sections are much smaller, making the interpretation easier (one can generally ignore multiple scattering), but the experiment is more difficult. In particular, the weak scattering leads to weak surface contributions to the scattering signal, so one must measure these signals under conditions which minimize the scattering contributions from the underlying bulk. Basically this means measuring in regions of scattering vector (Δk) space where this is no bulk signal, notably at locations in the component of Δk parallel to the surface corresponding to (‘fractional order’) diffracted beams only arising from a longer-range periodicity of the surface, or by measuring intensities at values of the component of Δk perpendicular to the surface midway between the conditions for bulk reflections (‘rod scans’). The simpler underlying theory means that surface x-ray diffraction (SXR) can be used to address structures with much larger surface periodicity, and that one can benefit from Fourier transform methods (Patterson functions) that provide some direct information on the surface structure. Indeed, more sophisticated ‘direct methods’ have been developed for the treatment of SXR data that can prove far more effective than simple Patterson functions [8]. These methods reduce the reliance on trial-and-error modelling which is generally only required in structural refinement of the correct basic model. The weak scattering also means that SXR has the benefit of being able to provide information on the structure

of buried interfaces. On the other hand, SXR has a rather poor sensitivity to the location of atoms of low atomic number, Z , because the scattering cross-section scales as Z^2 . The need for a very bright source of x-rays also means the experiments require the use of synchrotron radiation.

This requirement for synchrotron radiation is also a feature of the two local electron scattering methods, photoelectron diffraction [9, 10] and surface extended x-ray absorption fine structure (SEXAFS) [11], as well as the hybrid technique of standing x-ray waves (SXW) [12, 13]; all these experiments require the ability to continuously vary the x-ray photon energy. Photoelectron diffraction and SEXAFS both exploit the elastic scattering of photoelectrons emitted from a core level of a surface atom by surrounding atoms, which interferes with the outgoing photoelectron wavefield. In SEXAFS this interference is detected at the emitter atom itself, as this modifies the total photoionization cross-section. The variation of this cross-section with photon energy (and hence photoelectron energy and wavelength) provides a measure of the round-trip distance the electrons travel from the emitter to near-neighbour backscattering atoms and back to the emitter. Typically, the primary information emerging from SEXAFS is the nearest-neighbour emitter–scatterer distance, and this information can be extracted rather easily. Despite the fact that the electron energies are similar to those in LEED, multiple scattering effects are not significant for this shortest backscattering pathlength. In photoelectron diffraction it is the photoelectrons themselves that are detected outside the surface in an angle-resolved fashion, so the scattering pathlength differences relative to the directly emitted electrons vary with collection angle, and one can probe the resulting interference by making either angle-scan or energy-scan measurements. Photoelectron diffraction thus involves measurement of a derivative photoelectron cross-section (with respect to angle) and the resulting modulation amplitudes are typically an order of magnitude larger than in SEXAFS (tens of % rather than a few %). The angle-resolved character allows one to determine not only the distances, but also the directions of emitter–scatterer bonds, in a rather direct fashion. This enhanced information can only be extracted, however, by the use of multiple scattering simulations in a trial-and-error fashion similar to that used in LEED. Special features of SEXAFS and photoelectron diffraction, relative to LEED and SXR, are the fact that they are local structural probes, that do not rely on long-range order, and that they are *element specific*; the emitter atom is identified by its core level photoelectron binding energy, so one determines the local structure around an atom of a specific elemental species. This aspect makes these techniques particularly valuable for studies of adsorbate systems and ultra-thin layers on surfaces. Photoelectron diffraction has the added benefit of *chemical-state specificity*; i.e. the ability to separate out structural information around emitter atoms of the same element but in different environments, through the use of ‘chemical shifts’ in the photoelectron binding energy. This makes this technique particularly well-suited to studies of more complex molecular and co-adsorbate systems. It is perhaps worth remarking that there have been quite a number of attempts to extend

the idea of direct methods of data inversion (as used in SXRD) to produce a real-space atomic-scale image of the surface structure based on both photoelectron diffraction and LEED intensity data. Note, in particular, that the angular distribution of photoelectron diffraction at a fixed energy can be regarded as a photoelectron hologram. There are, however, fundamental obstacles associated with the influence of multiple scattering and of energy- and angle-dependent phase shifts in electron scattering from atoms, neither of which are significant problems in SXRD. Some success has been claimed, particularly in LEED [8], but extensive applications of a simple inversion method on photoelectron diffraction data [14] suggests that even the most sophisticated attempts to circumvent this problem may fail to be effective for adsorbate atoms in low-symmetry sites relative to the substrate, as is common for molecular adsorbates.

This same elemental- and chemical-state specificity is also a feature of a 'hybrid' diffraction method, namely x-ray standing waves (XSW). In this technique one works near a conventional Bragg reflection condition of the crystalline solid and exploits the standing x-ray wavefield that is set up by the interference of the incident and diffracted beam. Scanning through the Bragg condition in x-ray wavelength causes the standing wave to shift in phase relative to the crystal in a controlled way, and if one monitors the photoabsorption in this wavefield at a particular atomic species during this scan, the resulting variation in absorption allows one to establish the location of the absorbing atom relative to the bulk atomic scatterer planes. Monitoring this local photoabsorption by the resulting photoemission spectrum provides one with the required surface-, elemental-, and chemical-state specificities. This method, too, provides local structural information of the absorber atom relative to the underlying (ordered) substrate, with no requirement for long-range order in the adsorbate layer.

The final group of experimental methods for quantitative surface structure determination are those based on ion scattering, typically H^+ and He^+ , though some heavier alkali and noble gas ions are also used. There are two rather different energy ranges of roughly 1–10 and 50–300 keV, that define the methods of low and medium energy ion scattering (LEIS and MEIS), respectively [15, 16]. The associated de Broglie wavelengths of these energetic and relatively massive particles are far shorter than typical interatomic distances, and the scattering can normally be described in purely classical terms as simple two-body ion-atom elastic collisions. The scattered ion energy for an experimentally-defined scattering angle provides a measure of the scattering atom mass, but the key structural information derives from shadowing effects that result from this elastic scattering, using simple triangulation of the angles at which atoms in different layers emerge from shadow cones. These shadow cones are narrower at higher energies, so MEIS offers the potential of higher precision in structural measurements, and also allows deeper subsurface penetration, thus permitting structural studies of shallowly-buried interfaces. Because the scattering cross-sections in this technique also scale at Z^2 , the technique is most favourable for the study of higher-mass-number materials; in structural problems involving adsorption involving low

atomic number atoms, its strength lies in its ability to provide information preferentially on adsorbate-induced movements of substrate atoms.

While these methods allow one to determine atomic positions at surfaces in a quantitative fashion, an important development in surface science in the last 20 years or more has been the increasing use of atomic-scale imaging using scanning probe methods and, in particular, scanning tunnelling microscopy (STM). If one can 'see' the atoms at a surface, why do we need these other complex and indirect methods of surface structure determination? The answer is twofold: first, the protrusions seen in an STM image do not always correspond to atomic positions, and not all surface atoms lead to such protrusions, and secondly there is no simple quantitative relationship between the height (or indeed the exact lateral positions) of these protrusions, and the positions of underlying atoms (e.g. [17]). The reason for both of these problems is that STM is a probe of the spatial variation of the electronic structure of the surface (which determines the probability of electron tunnelling between the surface and the tip), and not of the atomic positions. In some cases this relationship between these two is simple, in some cases it is complex. Despite this, STM does have a valuable role to play in surface structure determination. Firstly, the images clearly show the extent of surface inhomogeneity and the way this inhomogeneity may influence the results of the (spatially-averaging) quantitative methods summarized above. In addition, atomic-scale images, and the evolution of these images during the formation of surface structures resulting, for example, from adsorption, may give important clues as the most promising structural models to be tested by the quantitative methods.

Finally, it is important to comment on the role of theoretical total energy calculations. As remarked in the introduction, DFT calculations, in particular, have been very successful in reproducing the main results of experimental surface structure determinations, and have an important role in helping to understand surface structural phenomena. They are, however, becoming used increasingly as a primary method of surface structure 'determination', and in evaluating data obtained in this way it is important to understand some intrinsic limitations. The first is that these methods are based, like almost all experimental surface structure determinations, on a trial-and-error approach. The associated computer programs incorporate sophisticated algorithms to determine the values of the structural parameters that lead to the lowest energy structure for a specified model (although, as in the experimental studies, it is possible to converge on a local, rather than the global, minimum in a complex multi-parameter space). More important, though, is the fact that these methods also only find the true lowest energy structure if the correct structural model is tested. Different structural models may, for example, involve different number of atoms within a surface unit mesh, and the search algorithms cannot switch between models of differing stoichiometry. Application of these calculations thus suffers from exactly the same limitation as the experimental methods; the final structural solution is constrained by the imagination of the researcher. The second

issue concerns accuracy and precision. There is at least one clearly-established failure of standard DFT codes to correctly determine the relative energies of two distinct structural models for an adsorption structure; for CO on Pt(111) (and on Rh(111)) there is clear experimental evidence that at low coverages CO adsorbs in singly-coordinated atop sites, yet calculations show the three-fold-coordinated hollow site to have the lower energy [18–21]. With hindsight, modifications to the theory can yield the correct energetic ordering, but this makes the ‘*ab initio*’ character of the calculations questionable. Moreover, there are a number of examples in which structural parameter values, notably chemisorption bondlengths, differ from experimental values by significantly more than the estimated precision of the experiment (typically $\sim 0.02\text{--}0.05$ Å). In effect, therefore, both results indicate that there may be unknown systematic errors associated with these computational codes. Experiments, of course, are also subject to errors, but in this case the random errors can be estimated by well-established methods, and systematic errors can usually be eliminated by careful comparisons of different methods on model systems. It is also important to recognize that DFT calculations usually take no account of finite temperature, in effect calculating internal energies rather than free energies. All of these factors are important reminders that such calculations (for which no error estimates can be offered) should not be regarded as invincible, despite their very considerable value in complementing experimental studies.

3. Surface structure—basic phenomenology

Surface structural phenomena can be loosely categorized as relaxation, reconstruction and adsorbate-related issues. Compared to a bulk solid, a surface has half of the atoms replaced by vacuum, and we can expect this to have some consequence for the exact positions of the atoms in the outermost surface layers. In particular, one might expect that the interlayer spacing of the outermost layers will differ from those of the underlying bulk, due to the removal of the atoms above them. This relaxation is the only structural modification that occurs at most low-index metal surfaces, and the direction is inwards (towards the bulk) and is largest from the most open-packed surfaces. For simple metals the bonding is non-directional and the interatomic distance in the bulk corresponds to an optimal value of the valence electron charge density. At a surface, this electron charge spills out some way into the vacuum, depleting the charge at the atomic ion cores, and these atoms are then displaced inwards towards a region of higher charge density in order to lower the total energy. Very careful measurements indicate that this general relaxation effect can propagate in a heavily damped fashion below the surface with alternating sign, such that, for example, the second-to-third layer spacing is expanded by an amount significantly smaller than the outermost layer contraction. This effect may, in part, be related to weak damped fluctuations (Friedel oscillations) in the electron charge density as a function of depth below the surface, although the structural effect is predicted to occur even in theoretical treatments that do not allow Friedel oscillations [22]. The typical magnitude of the

surface layer contraction in fcc metals on the most open-packed (110) surface is around 10%, while for the most closely-packed (111) surface the effect is marginally detectable (probably no more than 2%, and there has even been some debate in the literature regarding the sign of the relaxation in this case). As a specific example, LEED measurements from Al(110) indicate a surface layer contraction of 8.5%, a second layer expansion of 5.5%, and a third layer contraction of 1.5%, each with an estimated precision of approximately 1% [23].

More radical changes in the structure of a surface, relative to the structure to be expected from an ideal bulk termination, are usually referred to as reconstruction. In general these involve movement of atoms parallel to, as well as perpendicular to, the surface, and in many cases the atomic density of the surface layer or layers differs from that of the underlying bulk. Changes of this type are perhaps most easily understood for solids in which the bonding is predominantly or exclusively covalent, implying high localized directional bonds. The classic examples are elemental silicon and germanium. The simplest such case is that of Si(100). In an ideal bulk termination each surface Si atom has two ‘dangling bonds’; it is bonded to two Si atoms in the layer below but is missing two neighbours above due to the creation of the surface. The result is that adjacent pairs of surface Si atoms move together to form dimers, reducing the number of dangling bands per surface atom to one, rather than two. While this basic pairing was understood at an early stage and easily reconciled with a doubling of the periodicity of the surface unit mesh in one direction, relative to that of the underlying substrate—a (2×1) periodicity is seen in both LEED and STM—the full details of this reconstruction emerged somewhat later (e.g. [24]). Specifically, the surface dimers are asymmetric, with the Si–Si bond tilted relative to the surface, but at room temperature there is a dynamic flipping of the dimer between the two opposite asymmetric states, with only the average atomic positions being monitored by these methods (figure 1). At low temperature, however, this flipping is suppressed and a longer-range ordering of the asymmetric dimers can arise, leading to a $c(4 \times 2)$ periodicity, although some details of this asymmetry and ordering have proved controversial, even quite recently [25].

By contrast, Si(111), at which ideal bulk termination leads to just one dangling bond per surface atom, pointing perpendicularly out of the surface, proved far more complex to understand, not least because the surface reconstruction leads to a (7×7) unit mesh with an area 49 times that of the underlying bulk. In the 1970s, in particular, there were very many proposed solutions to this problem which briefly entered the realms of ‘speculative physics’, but it was the group of Takayanagi and co-workers, based on measurements using high energy electron diffraction (not a technique generally considered as a surface structural method) that led to the solution [26] that is now generally accepted as correct. This so-called DAS model has three key ingredients, namely Dimers, Adatoms, and a Stacking fault over one half of the surface unit mesh. The dimers involve pairing of adjacent surface Si atoms, exactly as on the (100) surface, although on the (111) surface the fact that the unreconstructed surface has

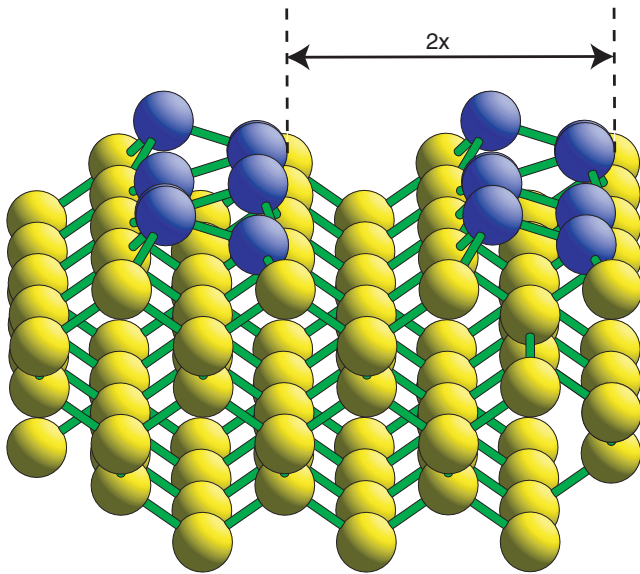


Figure 1. Schematic perspective view of the Si(100) surface showing the (2×1) ordering of the surface Si dimers but the disorder of their asymmetry. The outermost (dimerized) Si atoms are shown in a different shading for clarity.

only one dangling bond per surface atom means that this pairing nominally removes completely the dangling bonds of the dimer atoms. The benefit of the adatoms—‘extra’ Si atoms on the surface relative to the ideal bulk termination, may be appreciated by noting that the outermost bulk-terminated layer has hexagonal packing, with each Si atom having three bonds to Si atoms in the layer below and one dangling bond. Adding an extra Si adatom midway between three nearest-neighbour surface atoms thus saturates all three of these dangling bonds, and leaves the adatom with its own single dangling bond—but replacing three dangling bonds by one clearly leads to a reduction of the surface energy. It is this combination of dangling bond reduction through dimerization and adatom addition that is the primary source of energy reduction that drives this complex reconstruction. Of course, one might ask: where do the adatoms come from? In truth, this is a generic problem in the large number of surface reconstructions of many materials that involve changes in the areal density of atoms in the surface. The answer is that atoms simply diffuse over the surface, the necessary sources or sinks of atoms being surface steps. On many metal surfaces surface mobility is very high, even at room temperature. On Si surfaces the room temperature mobility is low, but the well-ordered (7×7) reconstructed (111) surface is only obtained after elevated temperature annealing. Indeed, if one cleaves bulk Si, to expose (111) facets, this surface does not show the (7×7) reconstruction, but a metastable (2×1) phase.

The third general class of materials with distinct surface structural phenomena are ionically-bonded solids. Structurally, at least, the simplest such materials that have proved of interest in surface science are the oxides having the rock salt structure, such as MgO and NiO. For these materials a key issue governing the stability of the surface is polarity. Within the bulk, atomic planes of certain orientations (notably (100))

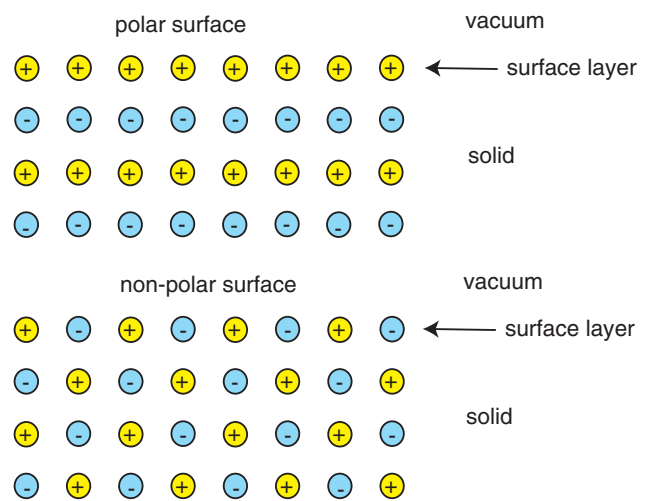


Figure 2. Schematic side view of simple polar and non-polar surfaces of ionic solids.

contain equal numbers of cations and anions and are thus electrostatically neutral, whereas other orientations comprise alternate layers of different stoichiometry, most notably the (111) planes that are alternately all anions and all cations. The consequences for the surfaces of these orientations are shown schematically in figure 2. While the first type of orientation leads to a non-polar surface, the second produces a polar surface, and the termination of the polar surface leads to a divergent energy associated with the surface dipole–dipole interactions. Such a surface must, therefore, be intrinsically unstable. For these solids the (100) surface is therefore stable and essentially bulk-terminated, albeit with some relaxation perpendicular to the surface that differs for the anions and cations. The (111) surfaces, however, do appear to be unstable, and figure 3 shows the ‘octopolar’ reconstruction that has been generally favoured as the model for the (2×2) reconstruction of NiO(111), first proposed on the basis of theoretical energy considerations [27]. This is a metal-terminated surface in which 3/4 of the surface Ni atoms, and 1/4 of the second layer O atoms, are missing, and as figure 3 shows this may be thought of as creating nanoscale (100) facets on the surface. The structure of these reconstructed surfaces is not, however, without controversy (e.g. [28–30]). In part, at least, this may be due to problems in preparing fully-characterized surfaces; the typical cycles of argon ion bombardment and annealing in ultra-high vacuum that work well for most metal surfaces and many semiconductors tend to leave poorly ordered and/or non-stoichiometric surfaces of these oxides, and much work nowadays is performed on thin epitaxial films that can be deposited and removed *in situ*. Moreover, the insulating character of these solids makes it difficult to use the standard methods of surface science, using electrons or ions, to investigate the properties of the surfaces of bulk crystals, due to surface charging; almost all the structural information has come from surface x-ray diffraction. Another issue is the possible hydroxylation of these surfaces due to interaction with hydrogen or water; hydrogen is, of course, difficult to detect by most surface science methods used for

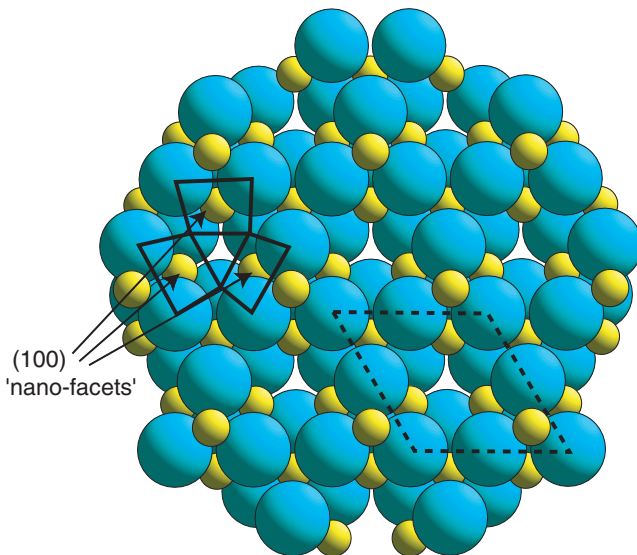


Figure 3. The ‘octopolar’ reconstruction model of NiO(111), showing the associated (100) ‘nanofacets’. The dashed lines define the (2×2) periodicity. The atoms are shown as spheres having the appropriate ionic radii, so the large spheres represent O^{2-} ions and the small spheres represent Ni^{2+} ions.

the characterization of surface composition. In the case of NiO(111), there is explicit evidence that an unreconstructed (1×1) surface is stable in the presence of surface hydroxyl species, and that the transformation to, and from, the clean surface (2×2) reconstruction, can be achieved reversibly by desorption and adsorption of molecular water [31].

Of course, not all oxides have this simple rock salt structure nor the 1:1 stoichiometry of the constituent elements, and no surface orientation may correspond to a stacking of charge-neutral atomic planes. It is also important to recognize, of course, that most solids are not only covalently or ionically bonded; for example, non-elemental semiconductors such as the III–V compounds with the zinc blende structure (with atomic positions like those of Si and Ge) also generally display at least some degree of ionicity. A general consideration that seems to determine the surface stability in many of these systems is then the concept of surface charge neutrality achieved by ‘autocompensation’; the flow of charge between cations and anions at the surface. This electron redistribution clearly leads to some structural relaxation, but may avoid the need for substantial lateral reconstruction of the surface. There seems to be generally a good level of understanding of many of the simpler reconstructions of compound semiconductors on this basis [32], although reconstruction is inevitably a consequence of non-stoichiometric ordered surfaces such as, for example, (100) surfaces of III–V semiconductors during different growth conditions in molecular beam epitaxy. This concept of autocompensation is also invoked to understand the stability of the unreconstructed rutile $TiO_2(110)(1 \times 1)$ surface, the most-studied oxide surface. In the bulk solid the constituent atoms are believed to have nominal Ti^{4+} and O^{2-} charge states, but despite the surface containing undercoordinated Ti and O atoms, electron spectroscopic data suggests these bulk charge states are retained, (despite undercoordinated Ti atoms at defect sites in the bulk appearing to have Ti^{3+} charge

states). The resulting surface structure does show relaxation of the atomic positions relative to an ideally-terminated bulk structure, but no major lateral reconstruction.

We should finally return to the rather few cases of true reconstruction of clean metal surfaces. As remarked above, most metal surfaces simply show small amounts of relaxation perpendicular to the surface, while the reconstruction of many non-metallic surfaces can be reconciled with the effects of directional dangling bonds, charge redistribution, and avoiding the particular problems of strongly polar surfaces. There are, however, a few cases of major reconstruction of clean surfaces. A particular case that can be understood, at least qualitatively, in terms of simple non-directional metallic bonding, is the case of Au(111). The bulk-terminated structure of this surface would comprise a close-packed layer of Au atoms, yet a reconstruction occurs in which the surface layer becomes slightly more close-packed by uniaxial compression, leading to a large-period commensurate surface layer with a $(23 \times \sqrt{3})\text{rect.}$ surface mesh [33–35]. Why should a close-packed metal surface, typically the most stable configuration, reconstruct? The answer is related to the valence charge depletion that occurs at the surface layer of a metal, due to spill-over into the vacuum, already discussed at the beginning of this section. One response to this is for the surface layer to relax inwards a little towards the bulk. Another way that the surface atoms could increase their surrounding valence electron charge density would be to move closer to their neighbours within the surface layer, but each surface atom occupies a well in the laterally-corrugated potential determined by interaction with the underlying metal atom layer. The general consequence of this is that the surface layer of a metal is in tensile surface stress—the atoms would like to move closer together (as they would in bulk tensile strain), but are unable to do so because of this laterally-corrugated potential. Whether or not the atoms move laterally, of course, depends on the relative magnitude of the surface stress and of the corrugation amplitude of the surface potential. On Au(111) the surface stress is sufficient to drive this reconstruction. Interestingly, a similar reconstruction to an approximately hexagonal close-packed surface layer occurs on Au(100), a more open-packed surface upon which the corrugation amplitude of the substrate may be expected to be larger, as is the change in atom areal density of the surface layer. By contrast, the Au(110) surface, in common with a few other fcc(110) metal surfaces, reconstructs by reducing the density of Au atoms in the outermost surface layer by 50%, but the resulting structure then displays close-packed (111) nanofacets, which, as a result of a large ($\sim 20\%$) inwards relaxation of the resulting surface layer [36, 37] effectively increases the atomic density within these nanofacets to a value higher than in a bulk-terminated (111) surface.

While many of these relaxation and reconstruction phenomena in metals, semiconductors and oxides can thus be understood, and least in general terms, with simple physical models, there are certainly a few systems for which the rationale is far less transparent. Notable examples are the cases of W(100) and Mo(100); in both cases, reconstructions involving significant lateral movements of the surface atoms occur, although the surface layer atomic density

is unchanged. It is tempting to think of this as a consequence of dangling bond effects in these more complex d-band metals, but while quantitative theoretical treatments reproduce the reconstructions [22], no simple physical picture emerges.

4. Adsorption at surfaces

4.1. Atomic adsorbates

While the structure of clean surfaces is of fundamental interest, most surface phenomena of practical importance, such as heterogeneous catalysis and device fabrication, relate to the interaction of atoms and molecules with surfaces. Understanding the structural aspects of adsorbates on surfaces, such as the adsorption site, the adsorption bondlengths, and the way the interaction of the adsorbates and the surface may modify one another, are thus key questions. Because of their relative simplicity, most early structural investigations of adsorption were of atomic adsorbates, studied at sub-monolayer coverages. On metal surfaces the early focus was on oxygen adsorption, followed by sulfur and other chalcogens, and by halogens and alkali atoms [5]. There has also been quite a number of studies of metal-on-metal systems, many related to interest in epitaxial growth, but also in alloy formation. For those systems in which the adsorbed atoms occupy sites on the surface (as opposed to in the surface—see below), much the most common phenomenon is of adsorption in the maximally-coordinated surface site—effectively the site that one would obtain from a simple billiard-ball model with no regard to the character of the bonding. On most surfaces, these are also the sites that would be occupied by the next layer of the substrate material. In many of these systems the modification of the substrate structure is minimal, only introducing minor changes to the (often local) surface relaxation. Moreover, while the structural precision of some of the early experimental studies was inferior to that now commonly obtained, it was already possible in the mid-1980s to identify trends in the resulting adsorbate–substrate chemisorption bondlengths with the bond order (defined by the adsorbate–substrate coordination) in a Pauling-like relationship [38, 39]. Even for overlayer adsorption on metal surfaces, however, this simple situation is not universal. In particular, adsorbates (particularly oxygen) may adopt lower-coordination sites, and this adsorption may cause reconstruction of the surface.

A particular example is that of oxygen adsorption on the (110) and (100) surfaces of Cu, on which the adsorption leads to a significant (atom-density-lowering) reconstruction of the outermost metal layer, and the creation of a very similar local oxygen bonding geometry on the two surfaces. Specifically (figure 4), the structures can be regarded as resulting from the removal of alternate [001] Cu atoms rows on the (110) surface (e.g. [40]), and every fourth such row on the (100) surface [41–44]. On the (110) surface the oxygen atoms occupy long-bridge sites midway between the Cu atoms in the remaining surface [001] rows, while on the (100) surface the oxygen atoms occupy similar locations in the Cu[001] rows adjacent to the missing rows. Interestingly, this reconstruction of the Cu(100) surface leads to a local structure next to the

missing row similar to that of the atom rows at the step edge on Cu(410) [45], a surface that comprises a regular array of (100) terraces separated by atomic steps (figure 4). This surface is particularly stable in the presence of adsorbed oxygen, and many Cu surfaces that are vicinal to (100) facet to (410) when exposed to oxygen. While these equilibrium structures have been fully solved by conventional quantitative surface structural methods (particularly LEED, SXRD, and PhD), STM studies have added considerable insight into how these reconstructions form. In particular, while we have described the (110) reconstruction in terms of missing rows of Cu atoms, STM studies show that the formation of this structure is by added $-\text{Cu}-\text{O}-\text{Cu}-\text{O}-$ rows that grow out from the steps at terrace edges [46]. Of course, the description of the final ordered equilibrium structure as missing or added rows is equivalent. STM studies also show, though, that the Cu(100) surface reconstruction really does form by extraction of 1/4 of the surface Cu atoms to create missing rows. These rejected Cu atoms form monoatomic islands on the surface, and measurements of the fractional area of these islands confirms the number of rejected Cu atoms.

In contrast to these examples involving adsorption on a surface, there are also two somewhat different situations that can lead to incorporation of adsorbate atom in the surface, namely the formation of surface compounds and surface alloys. From a structural point of view the distinction is marginal, and the difference in nomenclature typically reflects a difference in bonding character and ordering. Surface compound formation typically involves the formation of a stoichiometric compound between the adsorbate and substrate atoms with a structure that is identical or similar to that of a known bulk compound. In some cases, for example a range of silicides formed on silicon surfaces by many metal atoms, but also sulfides and chlorides on Ag and Cu surfaces, formed by interaction of the metal with S and Cl adsorbates, the surface compound may grow into multilayer films that may, or may not, be epitaxially related to the underlying substrate. Even for these systems, however, there are sometimes distinct structural phases involving only a single layer of the compound—a true surface phase.

The situation regarding surface alloying is somewhat different. Of course, if one deposits a thin layer of material A on material B, and A and B are fully miscible, one may expect strong intermixing to occur at a temperature sufficiently high to allow reasonable rates of diffusion; the system will move towards a state in which there is a true equilibrium between the surface and bulk composition, which could simply create a bulk homogeneous alloy. However, many bulk alloys do display preferential segregation of one component to the surface, so in these cases at least a partially-enriched alloy will occur at the surface. A particularly interesting case occurs in some systems in which the adsorbate and substrate species are immiscible in the bulk (or can sustain only a very dilute solid solution), yet the adsorbate atoms find it energetically favourable to occupy a substitutional site in the outermost atomic layer, creating a distinct ordered surface alloy phase. Quite a number of these systems, based on metals and semimetals on metallic surfaces, have been investigated [47]; a particular structural issue concerns the ‘rumpling’ of the surface alloy

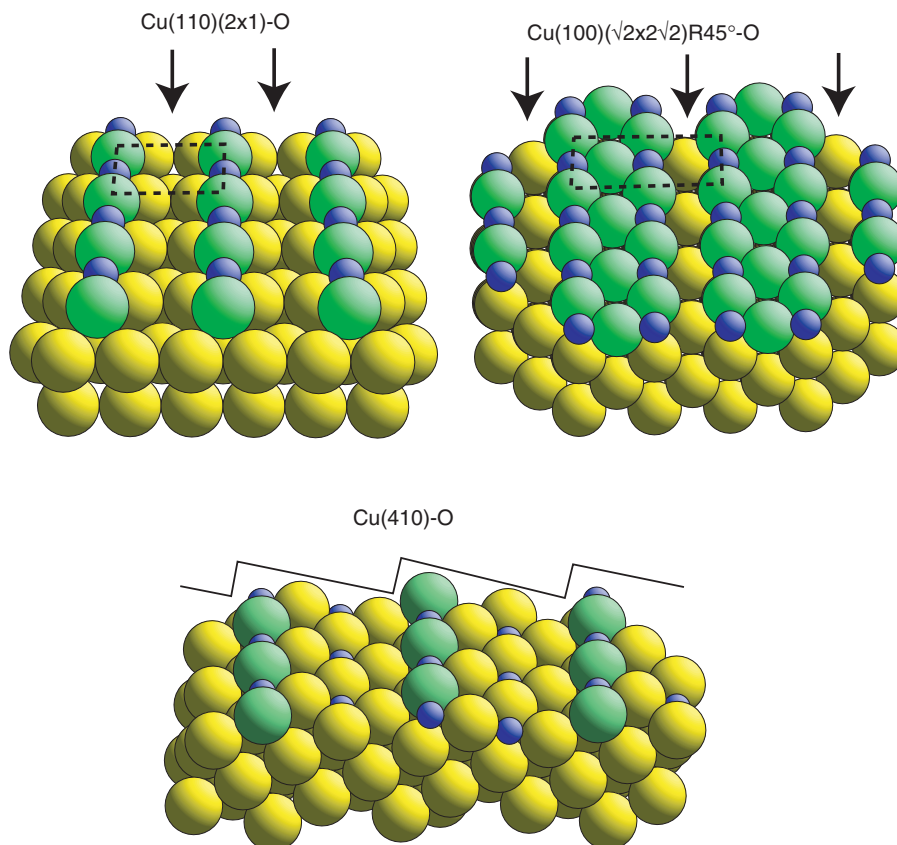


Figure 4. Schematic perspective views of the surface structures formed by oxygen adsorption on Cu(110), (100) and (410) surfaces. The O atoms are represented by the smaller spheres, while the shading of the outermost Cu atom layer (on the (410) surface these are the Cu atoms at the steps) differs from that of the underlying bulk for clarity. The arrows indicate the location of the ‘missing rows’ of Cu atoms, relative to the clean surface (bulk-terminated) structure. The dashed lines show the unit meshes of the reconstructed surfaces. The zig-zag line over the model of the (410) surface indicates the locations of the steps and terraces on this surface.

phase—i.e. the height difference above the substrate of the elementally-inequivalent atoms within the surface alloy. These surface alloys most typically seem to form in systems in which the adsorbate atom atomic radius is larger than that of the substrate species, so one would expect this adsorbate atom to have a significantly larger height above the substrate than the substrate atoms within the surface alloy layer, while this rumpling amplitude is commonly smaller than simple atomic radius arguments would imply. There is some evidence that this may be related to the fact that larger atoms in substitutional sites may reduce the tensile surface stress of the clean metal surface [48] discussed in section 3.

The energy balance between alloying and non-alloying behaviour can be quite subtle, as shown by the case of Bi on Cu(100) (figure 5). At low coverage a substitutional surface alloy is formed for which the geometry of the 0.25 ML $p(2 \times 2)$ phase has been determined by SXRD [49] and LEED [50]. At higher coverages, and notably in the 0.5 ML $c(2 \times 2)$ phase, dealloying occurs, and an overlayer structure is formed. Figure 4 shows the two structures with the Bi atoms drawn with radii chosen to just touch the Cu atom spheres (drawn with radii equal to half the interatomic spacing in the bulk). Presenting the structures in this way shows rather clearly the large effective radius change of the Bi atoms between these two phases. DFT calculations [48] yield total energies consistent

with this alloying/dealloying behaviour, and have also been used to evaluate the resulting changes in surface stress, though the extent to which this influences the total energy change is unclear.

So far this discussion of atomic adsorbate structure determinations has focussed on studies on metallic surfaces—this probably fairly reflects the numerical balance of such investigations. In particular, the great majority of studies of low atomic number atoms has been on metals. On covalently-bonded solids we have stressed the importance of the dangling bonds and their associated energies in determining the clean surface reconstructions, and one might imagine that adsorbates would readily form covalent adsorbate–substrate bonds at the remaining dangling bonds on the surface. This certainly does occur, particularly for molecular adsorbates, but on Si surfaces, for example, much of the emphasis of investigations of adsorption has been on deposition of metals and other semiconductors with a view to understanding the formation of contacts and semiconductor heterostructures; relatively little of this work has included full quantitative structure determinations. As remarked earlier, many metals form silicide compound phases on silicon surfaces, but one classic example of an overlayer structure involving metal atoms is the $(\sqrt{3} \times \sqrt{3})R30^\circ$ surface phase formed by deposition of 1 ML of Ag atoms, which are located at the dangling

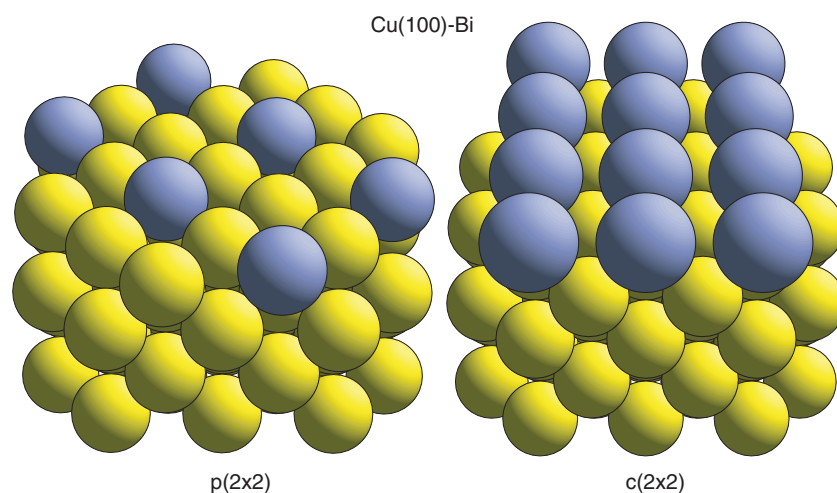


Figure 5. Schematic perspective views of the surface structures formed by bismuth adsorption on Cu(100). At a coverage of 0.25 ML a primitive (2×2) ordered phase is formed in which the Bi atoms occupy substitutional sites in the surface, but at a higher coverage of 0.5 ML the resulting centred (2×2) phase is de-alloyed, with the Bi atoms occupying four-fold coordinated hollow sites on the surface. The Cu atoms are represented by spheres with a radius equal to half the bulk interatomic spacing. The Bi atoms are shown as spheres with radii chosen to just touch the Cu spheres.

bond sites of the resultant outermost Si atoms. Top and side views of the resulting structure are shown in figure 6, with the atoms represented by small spheres in order that the network of interatomic bonds can be displayed. As is clear from the side view, the Si(111) substrate structure comprises narrowly-spaced double layers of Si atoms, and the Ag atoms, in effect, substitute the outermost half-layer Si atoms, while the lower half-layer forms Si trimers that give rise to the increased surface periodicity relative to an ideal bulk termination. The structure, known as the honeycomb chained trimer model, also involves significant surface and subsurface relaxation and was also solved by SXR [51] and LEED [52] studies.

4.2. Molecular adsorbates

The idea that adsorbates may attach to dangling bonds at the surfaces of covalently-bonded solids is particularly clear in studies of a number of molecular adsorbates in Si surfaces. Examples of this arise from the interaction of molecular water and ammonia with Si(100). As remarked in section 3, the clean Si(100) surface comprises Si dimers to reduce the number of dangling bonds, but each dimer atom retains a single dangling bond. Both water and ammonia dissociate on the surface, giving up one H atom, and both the H atom and the remaining hydroxyl (OH) [53] and amine (NH₂) [54] species attach to the Si dangling bonds; the dimers are retained, although it appears that their asymmetry is removed or, at least, reduced (e.g. figure 7). This statement should, perhaps, carry a caveat. None of the methods of surface structure determination show significant sensitivity to the location (or presence) of H atoms: they are extremely weak scatterers of both x-rays and electrons, and the H atom possesses no core level that can be used as a basis for photoelectron diffraction or SEXAFS. In these two molecular adsorption systems, therefore, the local geometry of the surface Si atoms and the O and N adsorbate atoms can be established, and the presence of a surface Si–H bond can

be inferred from vibrational spectroscopy, but the geometrical site of the adsorbed atomic H cannot be determined explicitly. Indeed, it is for this reason that investigations of the structure of atomic hydrogen on Si(100) were not discussed in the previous section; it is known that atomic H adsorbs on this surface. Indeed it is known that two distinct structural phases exist, referred to as monohydride and dihydride, at nominal coverages of 1 and 2 ML; in the monohydride the Si dimers are retained, while in the dihydride the dimer bonds are broken and the resulting structure has the (1×1) periodicity and structure of an essentially ideally bulk-terminated solid [55]. These observations clearly imply that the H atoms occupy dangling bond sites, but the H atom sites have not actually been determined experimentally.

Similar preferred attachment to the dangling bond sites have been confirmed for NH₃ dissociation fragments on the far more complex Si(111)(7×7) structure [56], and for hydrocarbons on Si(100). The simplest example of this latter group is ethylene (C₂H₄) on Si(100); the C–C bond lies above and parallel to the (symmetric) Si surface dimers [57], allowing a classic di- σ bonding to the Si dangling bonds.

On metal surfaces, much the most-studied molecular adsorbate in surface science is CO, motivated by the desire to understand a number of technologically significant cases of heterogeneous catalysis, and quite a number of these systems have also been the subject of structural studies. Unlike atomic adsorbates on metals, CO does not generally occupy maximally-coordinated sites on the surface, but more commonly forms local bonds of essentially covalent character, mimicking the behaviour in metal carbonyl complexes. Indeed, CO most commonly adsorbs on transition metal surfaces in singly-coordinated or doubly-coordinated atop or bridging sites, although there are also some systems in which three-fold coordinated sites are occupied (see below). The close analogy of the bonding of CO to these metal surfaces and in metal carbonyls was a major reason why vibrational spectroscopy

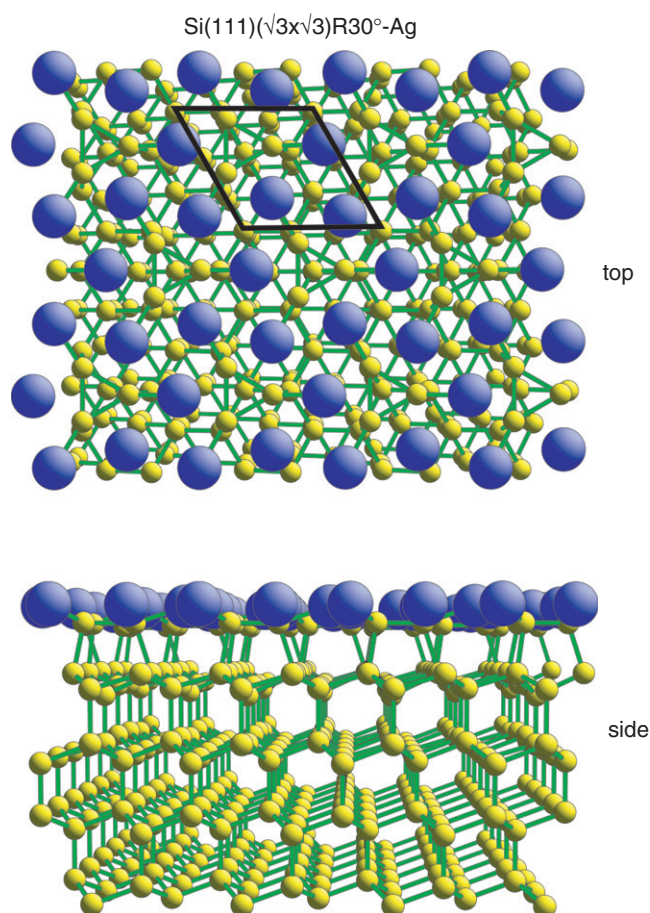


Figure 6. Top and side views of the ($\sqrt{3} \times \sqrt{3}$)R30° surface phase formed by deposition of 1 ML of Ag atoms onto Si(111). The atoms are represented by small spheres in order that the interatomic bonds can be displayed clearly. The surface unit mesh is marked on the top view.

has been widely used in isolation to identify adsorption sites on surfaces. This method relies on the fact that the C–O stretching frequency decreases in a systematic fashion as the metal coordination increases, and specific frequency ranges have been associated with specific bonding coordination, based on the known behaviour in metal carbonyls [58]. This approach is not without its problems, however, and a particular case of its failure is the $c(4 \times 2)$ phase formed by CO on Ni(111) (and also on Pd(111)). Based on an assignment of the C–O stretching frequency as characteristic of occupation of a bridging site, a very plausible structural model—in which the CO forms a regularly-spaced overlayer occupying symmetrically-inequivalent bridging sites (figure 8(a))—was widely accepted. Subsequent full structure determination for this system, however, using SEXAFS [59], photoelectron diffraction [60], and then LEED [61], has shown that in this phase CO actually occupies three-fold coordinated hollow sites, and specifically equal occupation of the two distinct such sites on an fcc(111) surfaces directly above second and third layer substrate atoms (so-called hcp and fcc hollows), as shown in figure 8(b). With hindsight, it is possible to reconcile the vibrational spectroscopic data with this revised model, but this example does highlight the danger of relying too heavily

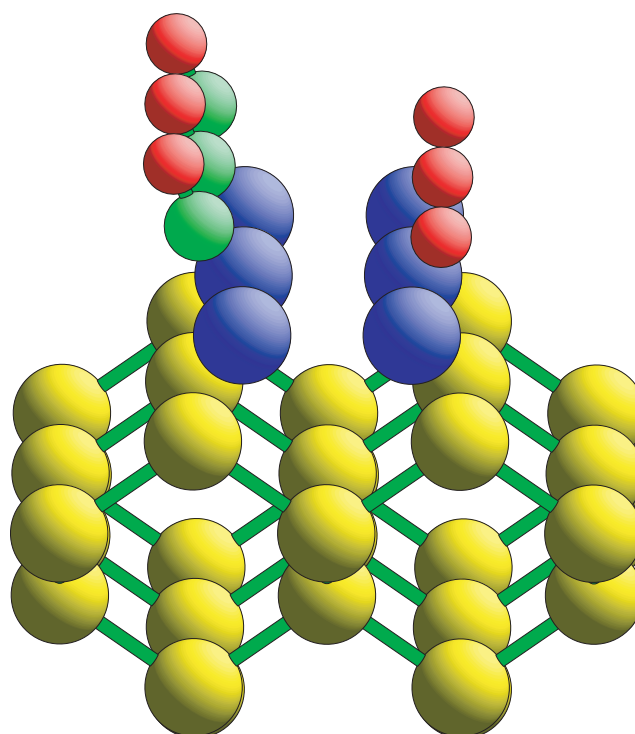


Figure 7. Schematic perspective view of the surface structure formed by water dissociation on Si(100) to produce coadsorbed OH and H. The outermost (dimerized) Si atoms are shown with a different shading to those of the bulk (as in figure 1) while the H atoms are represented by the smallest spheres. Note that it is not known whether the OH and H atoms are as well ordered at opposite ends of the Si dimers as shown in this representation.

on spectroscopic ‘fingerprinting’ to identify aspects of surface structure. The Ni/CO system has also been used as a model to investigate the relationship between bondlength and bond order for this molecular chemisorption system, comparing the structure of CO on Ni(100) and Ni(111) in different phases leading to singly-, doubly- and triply-coordinated adsorption sites. As for the atomic adsorption systems, this study also led to a Pauling-like relationship between these parameters, with the Ni–C bondlength increasing by $0.15 \pm 0.04 \text{ \AA}$ in decreasing the bond order from 1.0 to 0.5, and a further increase of $0.05 \pm 0.04 \text{ \AA}$ when the bond order is decreased to 0.33 [62].

This tendency to form local bonds at low-coordination sites is a feature of quite a number of molecular adsorbates on metal surfaces, and applies not only to diatomics, such as CO, NO and N₂, but also to more complex molecules. For example, the formate species, HCOO (formed by surface deprotonation of formic acid, HCOOH), is found to form local O–Cu singly-coordinated bonds on both Cu(110) and Cu(100), the molecular plane being perpendicular to the surface with the two O atoms near-atop two nearest-neighbour surface Cu atoms [63]. This same geometry is adopted by larger carboxylate species, notably acetate (CH₃COO) [64] and benzoate (C₆H₅COO) [65] on Cu(110), while even deprotonated simple amino acids, glycine (NH₂CH₂COO) [66] and alanine (NH₂CH₂CHCOO) [67] bond to this surface through the carboxylate O atoms, each in a similar singly-coordinated fashion, although the amino N atoms also

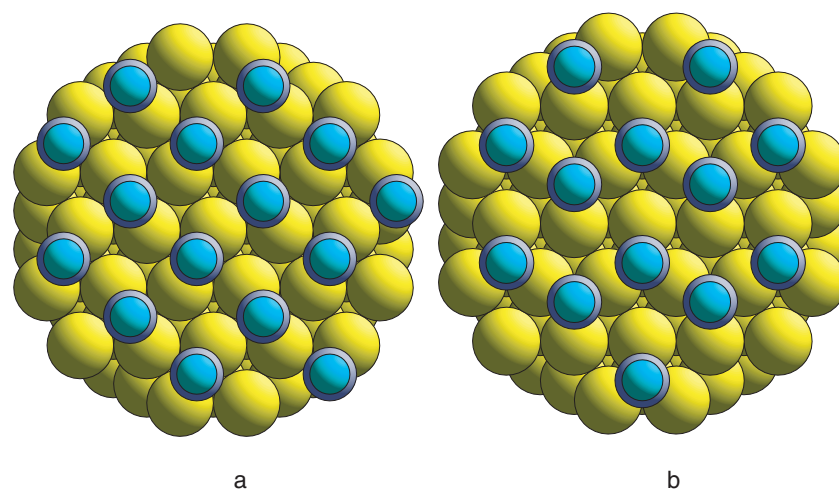


Figure 8. Top views of structural models of the Ni(111)c(4 × 2)-CO structure. (a) shows the original model based on vibrational spectroscopy which was interpreted in terms of occupation of bridging sites. The CO molecules are equi-spaced within a periodic mesh, but occupy symmetrically-inequivalent bridging sites relative to the substrate. (b) shows the result of quantitative structural studies in which the CO molecules occupy two inequivalent three-fold coordinated hollow sites, and are thus no longer equi-spaced.

adopt near-atop sites on surface Cu atoms (figure 9). The fact that the molecule ‘lies down’ to achieve this actually means that the O atoms are significantly further displaced from true atop sites in these systems due to the mismatch of the intramolecular O–N and surface Cu–Cu distances, but the bonding coordination is unchanged.

While there are, as yet, very few quantitative experimental studies of the structure of molecular adsorbates on oxide surfaces, there is certainly evidence of a similar tendency to form local molecule/surface-atom bonding. For example, CO, NO and NH₃ are all found to bond to NiO(100) surfaces atop the surface Ni atoms, thus forming local singly-coordinated bonds [68]. Moreover, on the rutile-phase TiO₂(110) surface (the most-studied of all oxide surfaces), it appears that carboxylic acids deprotonate and bond through the two carboxyl O atoms in near-atop sites to surface metal (Ti) atoms in a very similar fashion to that seen on Cu(110). However, on TiO₂ the surface O atoms form a more stable site for adsorption of the acid H atoms to form hydroxyl species. This geometry has been firmly established for the formate species on this surface [69], and also, most recently, for the glycinate species [70]. A key difference between glycinate on Cu(110) and TiO₂(110), however, is that this species does not ‘lie down’ on TiO₂ to form a metal-N bond, but this can be attributed, at least in part, to simple steric consideration associated with the different structure of the Cu and TiO₂(110) surfaces.

As a final example of molecular adsorption phenomena on surfaces, we consider a few cases involving essentially planar molecules. The simplest such molecule is benzene, C₆H₆, and it is well established that this molecule lies flat on most surfaces, at least a low coverages, interacting with the surface through the π -orbitals. The relatively delocalized character of these bonding orbitals might be expected to lead to a rather weak corrugation of the lateral surface potential that they experience, and thus to no strong preference for well-defined local adsorption site, and to high rates of surface diffusion. There is some indirect evidence to support this idea:

specifically, strong lateral ordering is seen on some surfaces only in the presence of coadsorbed CO. However, on Ni(111) a well-defined local adsorption geometry has been established by photoelectron diffraction even at low coverage with no long-range ordered phase. Interestingly, though, when the coverage is increased to 1/7 ML, at which an ordered ($\sqrt{7} \times \sqrt{7}$)R19° ordered phase is formed, both the local adsorption site and the azimuthal orientation of the molecule change (figure 10) [71]. In the ordered phase one can rationalize the new orientation in terms of steric effects, as the Van der Waals radii would overlap if the low coverage orientation was maintained in this ordering; the resulting structure is analogous to a set of six-toothed interlocking gear wheels. However, there is no comparable similar rationale for the local site change, nor for the preference of the other orientation at lower coverage. Of course, in some ways this result provides further evidence that the energetic differences between the different sites are subtle, and that the stable structures can be influenced by intermolecular interactions.

In the discussion of atomic adsorbates the issue of adsorbate-induced reconstruction of the substrate was discussed. This phenomenon also occurs in a few cases of molecular adsorbates; it seems, for example, that alkanethiols –CH₃(CH₂)_nSH– cause reconstruction of the (111) faces of the noble metals Cu, Ag and Au [72]. However, the inverse effect can occur with molecular adsorbates; adsorption may change the detailed structure of the adsorbate. In the case of benzene adsorption on surfaces, one obvious possible modification of this kind is an increase in the C–C bondlengths due to the interaction of the π -orbitals with the surface, and a consequential weakening of the C–C bonding. One might also expect some variation of the C–C bondlengths within the benzene ring to reflect the reduced (i.e. less than six-fold) rotational symmetry of the bonding site on the surface. In fact there is some evidence of both of these effects, but the precision with which one can determine the bondlengths parallel to the surface is marginally adequate

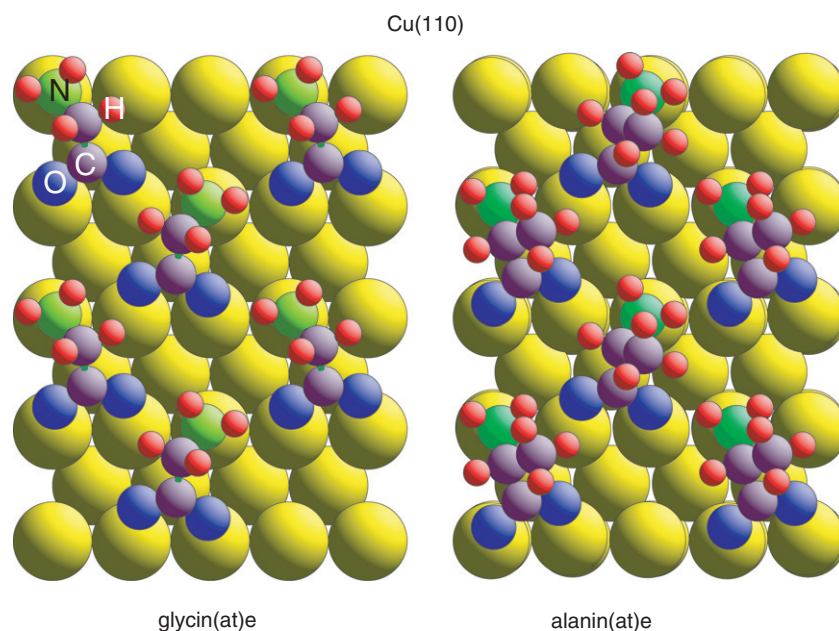


Figure 9. Schematic top view of the ordered structures formed by glycinate and alaninate (deprotonated glycine and alanine) on Cu(110). The actual structures shown are based on the results of DFT calculations; the photoelectron diffraction experimental studies determine the local adsorption sites of the constituent O and N atoms, but not the C and H atoms.

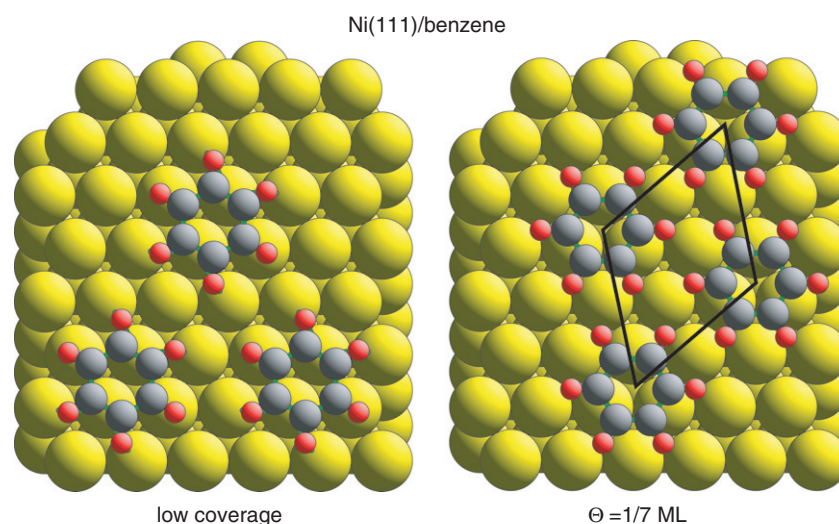


Figure 10. Schematic top view of the structures formed by benzene at low coverage, and a coverage of $1/7$ ML corresponding to the formation of an ordered $(\sqrt{7} \times \sqrt{7})R19^\circ$ phase. Note the change in azimuthal orientation and adsorption site (from bridge to hollow with increasing coverage). The full lines denote the nit mesh of the ordered overlayer phase.

to yield a statistically significant result [73]. LEED and photoelectron diffraction, in particular, the two methods that have been most used in these molecular adsorption studies, can achieve precision in distances perpendicular to the surface as small as 0.02 \AA , but parallel to the surface a lower limit of around 0.05 \AA is more typical. Adsorbate-induced C–C bondlength increases are, however, well established for the C_2 hydrocarbons acetylene (C_2H_2) and ethylene (C_2H_4) that bond to a number of metal surfaces, including Ni(111), with the C–C axis parallel to the surface [74]. Indeed, on this surface the C–C bondlength of adsorbed acetylene, with a bond order of three in the gas phase, increases to a value between that of gas-phase

ethylene and ethane, indicating a reduction of bond order to ~ 1.5 . A pronounced softening of the C–C stretching vibration is consistent with the geometrical effect.

A rather different manifestation of adsorbate-induced modification of the internal geometry of molecular adsorbates has been found quite recently from XSW studies of the structure of large near-planar molecules of very specific interest in molecular electronics. Specifically these experiments have studied NTCDA (1,4,5,8-naphthalene-tetracarboxylicacid-dianhydride) [75] and PTCDA (1,4,5,8-perylene-tetracarboxylicacid-dianhydride) [76] deposited on Ag(111), using O 1s photoemission to monitor the

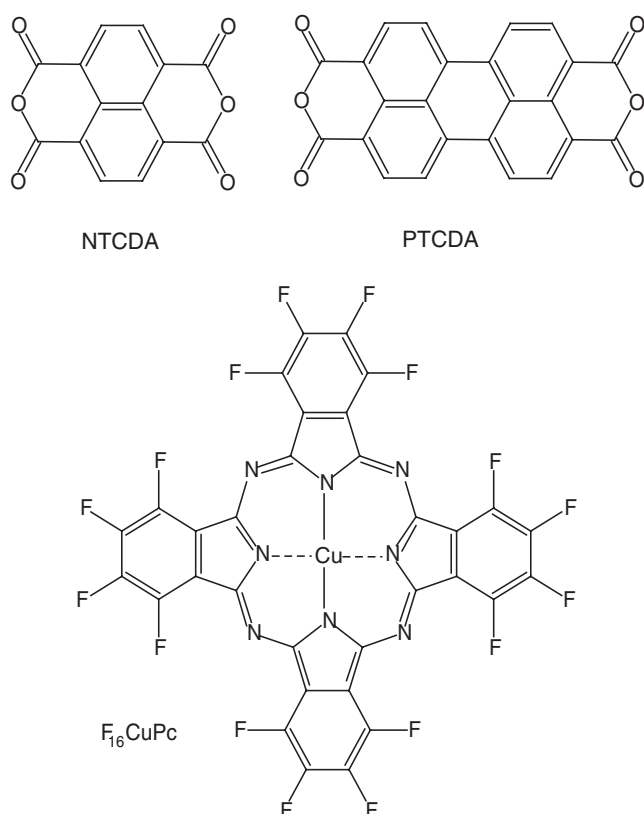


Figure 11. Structural formulae of the molecules NTCDA, PTCDA and $F_{16}CuPc$ described in the text.

location of the carboxylic acid O atoms on the perimeter of the molecules (see the structural formulae in figure 11). The layer spacing of the molecule above the surface gives information on the nature of the molecule–metal bonding, the value being short enough to imply chemisorption. However, in the case of the PTCDA molecule it also proved possible to obtain separate XSW profiles from the chemically-inequivalent O atoms (the four carboxylic O atoms at the corners and the two intermediate anhydride O atoms) through their photoelectron binding energy chemical shifts. This additional specificity provided further information on out-of-plane distortion of the adsorbed molecule giving rise to different heights of these atoms above the surface. A further example of this type of distortion has been seen in a study of the fluorinated copper phthalocyanine, $F_{16}CuPc$ (figure 11) adsorbed on Cu(111); in this investigation the different layer spacings of the F, N and C atoms of the molecule above the surface allowed the authors to gain insight into the buckling of the molecule induced by the adsorption [77].

5. Prospects and challenges

While surface structure determination is still very rarely ‘routine’, enormous progress has been made in the last 40 years since the very first demonstrations that experimental LEED intensity data from essentially known structures (the clean surfaces of Ni and Al) could be reproduced theoretically [78–81], paving the way for the determination of

new structures. Since then the number of available methods has blossomed, the ability to tackle more difficult systems has grown enormously (greatly helped by advances in computers) and a large number of structures have been solved [5]. What are the key challenges for the future? I believe there are two key issues: complexity and precision.

Surface science in general has, for some years now, been moving to problems of increasing complexity, extending well beyond simple atomic adsorption studies on low-index single crystal surfaces to investigation of complex reactions on a wide range of surfaces including deposited small particles and other nanostructures. With the exception of SEXAFS, all the quantitative structural methods discussed here are only applicable to single crystal surfaces although, of course, if one can achieve spatial resolution in the methods, to isolate individual grains in a sample that is polycrystalline or consists of individual small particles, this need not be a restriction. In this regard the potential to obtain LEED intensities from very small areas (down to a few nanometre) using a low energy electron microscope (LEEM) (e.g. [82, 83]) may be of crucial importance. For studies of extended single crystal surfaces there is a growing need to understand complex coadsorption systems (including reactants and reaction intermediates) that may occur in a surface catalytic reaction, and to characterize the interaction at a substrate surface of large molecules (such as those shown in figure 11) that are involved in molecular electronics. Ideally, one may wish to investigate surface reaction products under more realistic (i.e. non-UHV) pressures. Progress is being made on all of these fronts. Ambient pressure structural studies are possible—and are being performed (e.g. [84, 85])—using SXRD. Of course, SXRD is a technique that specifically exploits long-range order in the structure of interest, and complex co-adsorbate systems under reaction conditions may not generally show this long-range order. Local structural probes, and particularly photoelectron diffraction and photoelectron-detected XSW, with both element- and chemical-state specificity, are ideally suited to studies of these mixed surface phases—but only under the high vacuum conditions necessary for the emitted electron detection. Evidently, some combination of these methods under different conditions may be required to solve some of these problems.

Even for well-order surface phases of larger molecular adsorbates, there are significant challenges in achieving complete and reliable structure determinations. If one uses the local chemical-state specific methods, such as photoelectron diffraction and XSW, it is possible to determine adsorption structures in a piecemeal fashion, locating specific atoms relative to the surface in a largely independent fashion. On the other hand, the fact that interatomic distances in the adsorbed molecule and the substrate rarely match, means that at least some of the constituent atoms within the adsorbed molecule must occupy low-symmetry sites, and the fact that real measurements must then average over symmetry-equivalent domains relative to the substrate symmetry significantly reduces the potential precision of the methods. In practice, therefore, it is likely that constraints on the relative positions of the constituent atoms, based on the known structure of

the isolated molecule, may have to be imposed to obtain consistent unique solutions. The same conclusion arises in the use of conventional diffraction methods, such as LEED and SXRD, to tackle these problems. In the absence of elemental-and chemical-state specificity, it is improbable that a unique determination of the relative locations of all the atoms within a large adsorbed molecule can be achieved in an unconstrained fashion, and in practice an internal structure of the molecule that is heavily constrained may need to be imposed. Heavily-constrained solutions of this type have not, as yet, been widely used in surface structural studies, but it is important to recognize that in far more complex problems of conventional structure determination in solids, such as protein crystallography, the use of such constraints is standard practice.

It is perhaps evident from this discussion of the problems of tackling growing complexity, that advances in this area will generally lead to a loss of precision. As has been remarked earlier, the precision with which relatively simple structures can be solved, down to ~ 0.02 Å, is sufficient for real chemical significance; one can sensibly use interatomic distances with this precision to infer information about the character of chemical bonding. Even in these simpler systems, however, the current lower levels of precision that are sometimes obtained, notably in distances parallel to the surface, can lead to ambiguities in their chemical significance. For complex systems, with or without constrained solutions, precision will be a growing problem with no obvious general solution.

Despite these difficult challenges, however, it is clear that important progress is continuing to be made in surface structure determination in terms of complexity, ambient conditions, and spatial resolution. There seems to be no shortage of important but difficult problems that are coming within reach.

References

- [1] Andersson S and Pendry J B 1973 *J. Phys. C: Solid State Phys.* **6** 601
- [2] Demuth J E, Jepsen D W and Marcus P M 1973 *Phys. Rev. Lett.* **31** 540
- [3] Pendry J B 1974 *Low Energy Electron Diffraction* (New York: Academic)
- [4] Heinz K 1995 *Rep. Prog. Phys.* **58** 637
- [5] Watson P R, Van Hove M A and Hermann K 2003 *NIST Surface Structure Database Ver. 5.0* (Gaithersburg, MD: NIST)
- [6] Feidenhans'l R 1989 *Surf. Sci. Rep.* **10** 105
- [7] Robinson I K and Tweet D J 1992 *Rep. Prog. Phys.* **55** 599
- [8] Saldin D K and Shneerson V L 2008 *J. Phys.: Condens. Matter* **20** 304208
- [9] Woodruff D P and Bradshaw A M 1994 *Rep. Prog. Phys.* **57** 1029
- [10] Woodruff D P 2007 *Surf. Sci. Rep.* **62** 1
- [11] Stöhr J 1988 *X-ray Absorption, Principles, Techniques, Applications of EXAFS, SEXAFS and XANES* ed R Prins and D C Koeningberger (New York: Wiley) p 443
- [12] Zegenhagen J 1993 *Surf. Sci. Rep.* **18** 199
- [13] Woodruff D P 2005 *Rep. Prog. Phys.* **68** 743
- [14] Woodruff D P, Baumgärtel P, Hoelt J T, Kittel M and Polcik M 2001 *J. Phys.: Condens. Matter* **13** 10625
- [15] Niehus H, Heiland W and Taglauer E 1993 *Surf. Sci. Rep.* **17** 213
- [16] van der Veen J F 1985 *Surf. Sci. Rep.* **5** 199
- [17] Woodruff D P 2003 *Curr. Opin. Solid State Mater. Sci.* **7** 75
- [18] Feibelmann P, Hammer B, Nørskov J K, Wagner F, Scheffler M, Stumpf R, Watwe R and Dumesic J 2001 *J. Phys. Chem. B* **105** 4018
- [19] Gil A, Clotet A, Ricart J M, Kresse G, Garcia-Hernández M, Rösch N and Sautet P 2003 *Surf. Sci.* **530** 71
- [20] Kresse G, Gil A and Sautet P 2003 *Phys. Rev. B* **68** 073401
- [21] Köhler L and Kresse G 2004 *Phys. Rev. B* **70** 165405
- [22] Inglesfield J E 1985 *Prog. Surf. Sci.* **20** 105
- [23] Andersen J N, Nielsen H B, Petersen L and Adams D L 1984 *J. Phys. C: Solid State Phys.* **17** 173
- [24] Terakura K, Yamasaki T and Morikawa Y 1995 *Phase Transit.* **53** 143
- [25] Uda T, Shigekawa H, Sugawara Y, Mizuno S, Tochihiro H, Yamashita Y, Yoshinobu J, Nakatsuji K, Kawai H and Komori F 2004 *Prog. Surf. Sci.* **76** 147
- [26] Takayanagi K, Yanishiro Y, Takahashi M and Takahashi S 1985 *J. Vac. Sci. Technol. A* **3** 1502
- [27] Wolf D 1992 *Phys. Rev. Lett.* **68** 3315
- [28] Barbier A, Renaud G, Mocuta C and Stierle A 1999 *Surf. Sci.* **433** 761
- [29] Barbier A, Mocuta C, Kuhlenbeck H, Peters K F, Richter B and Renaud G 2000 *Phys. Rev. Lett.* **84** 2897
- [30] Erdman N, Warschkow O, Ellis D E and Marks L D 2000 *Surf. Sci.* **470** 1
- [31] Rohr F, Wirth K, Libuda J, Cappus D, Bäumer M and Freund H-J 1994 *Surf. Sci.* **315** L977
- [32] Duke C B 1993 *Appl. Surf. Sci.* **65** 543
- [33] Harten U, Lahee A M, Toennies J P and Wöll C 1985 *Phys. Rev. Lett.* **54** 2619
- [34] Huang K G, Gibbs D, Zehner D M, Sandy A R and Mochrie S G J 1990 *Phys. Rev. Lett.* **65** 3313
- [35] Barth J V, Brune H, Ertl G and Behm R J 1990 *Phys. Rev.* **42** 9307
- [36] Moritz W and Wolf D 1985 *Surf. Sci.* **163** L655
- [37] Vlieg E, Robinson I K and Kern K 1990 *Surf. Sci.* **233** 248
- [38] Mitchell K A R 1985 *Surf. Sci.* **149** 93
- [39] Mitchell K A R, Schlatter S A and Sodhi R N S 1986 *Can. J. Chem.* **64** 1435
- [40] Parkin S R, Zeng H C, Zhou M Y and Mitchell K A R 1990 *Phys. Rev. B* **41** 5432
- [41] Zeng H C and Mitchell K A R 1990 *Surf. Sci.* **239** L571
- [42] Atrie A, Bardi U, Casalone G, Rovida G and Zanazzi E 1990 *Vacuum* **41** 333
- [43] Robinson I K, Vlieg E and Ferrer S 1990 *Phys. Rev. B* **41** 6954
- [44] Kittel M *et al* 2001 *Surf. Sci.* **470** 311
- [45] Vlieg E *et al* 2002 *Surf. Sci.* **516** 16
- [46] Besenbacher F 1996 *Rep. Prog. Phys.* **59** 1737
- [47] Woodruff D P and Vlieg E 2002 *The Chemical Physics of Solid Surfaces* vol 10 *Surface Alloys and Alloy Surfaces* ed D P Woodruff (Amsterdam: Elsevier) p 277
- [48] Harrison M J, Woodruff D P and Robinson J 2004 *Surf. Sci.* **572** 309
- [49] Meyerheim H L, Zajonz H, Moritz W and Robinson I K 1997 *Surf. Sci.* **381** L551
- [50] AlShamaileh E and Barnes C 2002 *Phys. Chem. Chem. Phys.* **4** 5148
- [51] Takahashi T and Nakatani S 1993 *Surf. Sci.* **282** 17
- [52] Over H, Tong SY, Quinn J and Jona F 1995 *Surf. Rev. Lett.* **2** 451
- [53] Bengió S *et al* 2002 *Phys. Rev. B* **66** 195322
- [54] Franco N, Avila J, Davila M E, Asensio M C, Woodruff D P, Schaff O, Fernandez V, Schindler K-M, Fritzsche V and Bradshaw A M 1997 *Phys. Rev. Lett.* **79** 673
- [55] White S J, Woodruff D P, Holland B S and Zimmer R S 1978 *Surf. Sci.* **74** 34
- [56] Bengió S, Ascolani H, Franco N, Avila J, Asensio M C, Bradshaw A M and Woodruff D P 2004 *Phys. Rev. B* **69** 125340

- [57] Baumgärtel P *et al* 1999 *New J. Phys.* **1** 20
- [58] Sheppard N and Nguyen N T 1978 *Adv. Infrared Raman Spectrosc.* **5** 67
- [59] Becker L, Aminpirooz S, Hillert B, Pedio M, Haase J and Adams D L 1993 *Phys. Rev. B* **47** 9710
- [60] Schindler K-M *et al* 1993 *J. Electron Spectrosc. Relat. Phenom.* **64/65** 75
- [61] Mapledoram L D, Bessent M P, Wander A D and King D A 1994 *Chem. Phys. Lett.* **228** 527
- [62] Sayago D I, Hoeft J T, Polcik M, Kittel M, Toomes R L, Robinson J, Woodruff D P, Pascal M, Lamont C L A and Nisbet G 2003 *Phys. Rev. Lett.* **90** 116104
- [63] Woodruff D P, McConville C F, Kilcoyne A L D, Lindner Th, Somers J, Surman M, Paolucci G and Bradshaw A M 1988 *Surf. Sci.* **201** 228
- [64] Weiss K-U, Dippel R, Schindler K-M, Gardner P, Fritzsche V, Bradshaw A M, Kilcoyne A L D and Woodruff D P 1992 *Phys. Rev. Lett.* **69** 3196
- [65] Pascal M, Lamont C L A, Kittel M, Hoeft J T, Terborg R, Polcik M, Kang J H, Toomes R L and Woodruff D P 2001 *Surf. Sci.* **492** 285
- [66] Kang J-H, Toomes R L, Polcik M, Kittel M, Hoeft J-T, Efsthathiou V, Woodruff D P and Bradshaw A M 2003 *J. Chem. Phys.* **118** 6059
- [67] Sayago D I, Polcik M, Nisbet G, Lamont C L A and Woodruff D P 2005 *Surf. Sci.* **590** 76
- [68] Kittel M, Hoeft J-T, Polcik M, Bao S, Toomes R L, Kang J-H, Woodruff D P, Pascal M and Lamont C L A 2002 *Surf. Sci.* **499** 1
- [69] Sayago D I, Polcik M, Lindsay R, Hoeft J T, Kittel M, Toomes R L and Woodruff D P 2004 *J. Phys. Chem. B* **108** 14316
- [70] Lerotholi T J, Kröger E A, Knight M J, Unterberger W, Hogan K, Jackson D C, Lamont C L A and Woodruff D P 2009 *Surf. Sci.* **603** 2305–11
- [71] Schaff O, Fernandez V, Hofmann Ph, Schindler K-M, Theobald A, Fritzsche V, Bradshaw A M, Davis R and Woodruff D P 1996 *Surf. Sci.* **348** 89
- [72] Woodruff D P 2008 *Phys. Chem. Chem. Phys.* **10** 7211
- [73] Woodruff D P 2007 *Chemical Bonding at Surfaces and Interfaces* ed A Nilsson, L Pettersson and J Nørskov (Amsterdam: Elsevier) p 1
- [74] Bao S, Hofmann Ph, Schindler K-M, Fritzsche V, Bradshaw A M, Woodruff D P, Casado C and Asensio M C 1995 *Surf. Sci.* **323** 19
- [75] Stanzel J, Weigand W, Kilian L, Meyerheim H L, Kumpf C and Umbach E 2004 *Surf. Sci.* **571** L311
- [76] Hauschild A, Karki K, Cowie B C C, Rohlfing M, Tautz F S and Sokolowski M 2005 *Phys. Rev. Lett.* **94** 036106
- [77] Gerlach A, Schreiber F, Sellner S, Dosch H, Vartanyants I A, Cowie B C C, Lee T-L and Zegenhagen J 2005 *Phys. Rev. B* **71** 205425
- [78] Pendry J B 1969 *J. Phys. C: Solid State Phys.* **2** 2283
- [79] Tong S Y and Rhodin T N 1971 *Phys. Rev. Lett.* **26** 711
- [80] Demuth J E, Tong S Y and Rhodin T N 1972 *J. Vac. Sci. Technol.* **9** 639
- [81] Laramore G E and Duke C B 1972 *Phys. Rev. B* **5** 267
- [82] El Gabaly F, Puerta J M, Klein C, Saa A, Schmid A K, McCarty K F, Cerda J I and de la Figuera J 2007 *New J. Phys.* **9** 80
- [83] Hannon J B, Sun J, Pohl K and Kellogg G L 2006 *Phys. Rev. Lett.* **96** 246103
- [84] Steadman P, Peters K, Isern H, Alvarez J and Ferrer S 2000 *Phys. Rev. B* **62** R2295
- [85] Westerstrom R *et al* 2008 *J. Phys.: Condens. Matter* **20** 184018